The Evolution of Edge Vortices Underneath a Diffuser Equipped Bluff Body

by

S. Mahon [(1)], X. Zhang [(2)] and C. Gage

School of Engineering Sciences,

University of Southampton,

Southampton, SO17 1BJ, UK

[(1)]E-Mail: S.A.Mahon@soton.ac.uk

[(2)]E-Mail: X.Zhang@soton.ac.uk

ABSTRACT

The edge vortices generated by a diffuser equipped bluff body in ground effect were experimentally studied using a range of methods including particle image velocimetry (PIV), oil flow visualisation and forces. Two edge vortices were observed originating from each side of the diffuser caused by the flow separating off the side off the model and swirling underneath the model. The edge vortices were found to enhance the downforce generated by the model as the ride height was decreased. At low values of ride height the edge vortices broke down due to the streamwise pressure gradient within the diffuser becoming too severe. This impacted on the forces such that a reduction in downforce and increase in drag was observed. The vortices were generated close the diffuser inlet, evolving from regions of weak recirculation into concentrated vortices which moved inboard and vertically up as the location moved downstream.

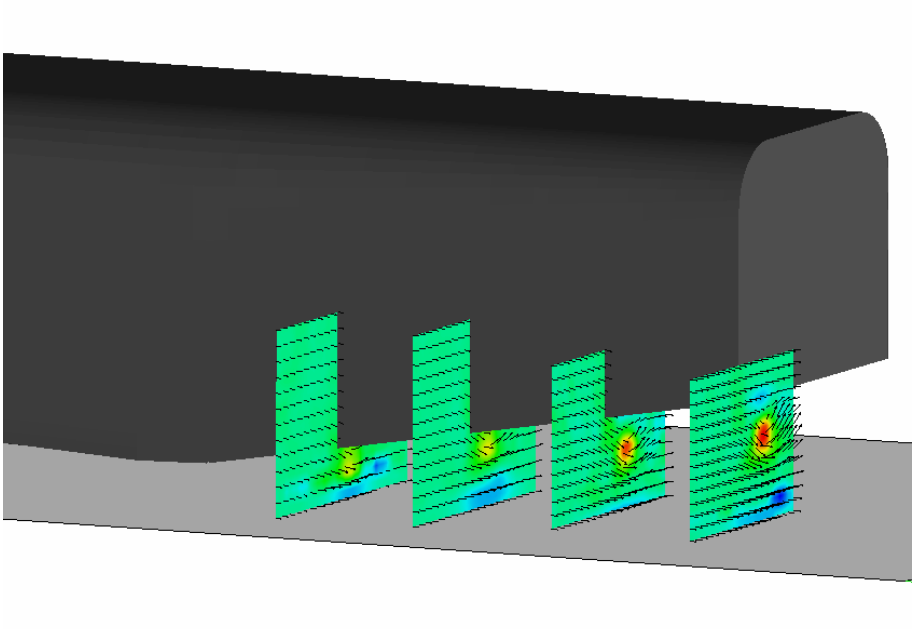

NOMENCLATURE

C_D	=	coefficient of drag, $D/q_\infty S$
C_L	=	coefficient of downforce, $L/q_\infty S$
d	=	model half-width, 0.157m
D	=	drag force
h	=	height of model, 0.324m
h_r	=	ride height
l	=	length of model, 1.315m
L	=	downforce
q_∞	=	freestream dynamic pressure, $?_\infty U_\infty{}^2/2$
Re	=	Reynolds number, $?U_\infty l/\mu$
S	=	frontal area of the model
U_∞	=	freestream streamwise velocity
u, v, w	=	streamwise, vertical and spanwise components of velocity
x,y,z	=	cartesian coordinates: x +ve downstream, y +ve up, z +ve to port
μ	=	viscosity
$?$	=	density
$?$	=	vorticity, $dv/dx-dw/dy$
O	=	non-dimensional vorticity, $? d/U_\infty$
$?$	=	diffuser expansion angle

1. INTRODUCTION

The performance of modern cars, both on the road and the racetrack, is strongly influenced by aerodynamics. Modern racing cars are designed to maximise the amount of negative lift (downforce) produced working in conjunction with the mechanical grip, to improve the acceleration, braking, and cornering speed of the car. Many aerodynamic devices are deployed to achieve this goal, the most obvious being inverted wings mounted at the front and rear of the car. Although less visible, shaping of the underside of the car is responsible for a large percentage of the total downforce generated.

There exists a lack of previous investigations into diffuser equipped bluff bodies. In 1981 Frost (Frost, 1981) investigated a bluff body with a rear diffuser in ground effect. Ramp angles of up to 20° were investigated without diffuser endplates. The flow visualisation indicated that the vortex formation occurred by the flow "rolling" around the side of the body to the underside of the ramp. This is obviously fundamentally different to diffusers with end fences, as the end fences would have prevented this flow pattern and method of vortex formation. Increasing the ramp angle had the effect of increasing the strength of the vortices. When the diffuser angle was increased to 20°, the vortices were no longer symmetric, but no breakdown occurred, and no flow separation was seen from the ramp surface. George (George, 1981) performed a similar study to Frost, and also concluded that the vortices prevented flow separation in the diffuser ramp. He went on to suggest that mounting vortex generators on the diffuser ramp would maintain vortex flow at low speeds, increasing the diffuser performance in conditions that would usually lead to vortex breakdown. This is outside the scope of the current investigation.

The studies carried out by Cooper *et al*. (Cooper *et al*., 1998; Cooper *et al*., 2000) in 1998 and 2000 involved a large number of tests using different diffuser settings and geometries. In most cases end fences were fitted to the diffuser. They found that interaction with the ground was a major source of downforce generation, and that the downforce produced varied significantly with ride height. They concluded that a diffuser with a small divergence angle reduces drag below that found when no diffuser is fitted. In the one test where the end fences were removed, they discovered more downforce was produced at very low ride heights than with end fences. Cooper *et al*. agreed with George that the introduction of a vortex into the diffuser ramp could be used to enhance its performance. Maximum

downforce was found to be produced when using a diffuser less than half the length of the bluff body, demonstrating that short diffusers provide the best performance. The lower the ramp angle, the shorter the diffuser ramp required for peak performance.

Most recently the investigations of Senior & Zhang (Senior and Zhang, 2001) and Ruhrmann & Zhang (Ruhrmann and Zhang, 2003) investigated a diffuser equipped bluff body in ground effect with end fences. Senior & Zhang observed the presence of two counter-rotating vortices that were recorded in previous studies (Cooper *et al*., 1998; Cooper *et al*., 2000). As in other studies, these vortices remained attached to the diffuser ramp, however the flow was seen to detach from the ramp surface just before the diffuser exit due to the adverse pressure gradient. Contrary to the fixed ground study by Burgin *et al*. (Burgin *et al*., 1986), reducing ride height was found to increase both drag and downforce. At the point of maximum force, the flow detached from the centre of the ramp surface, although the flow pattern remained symmetric. As the ride height was reduced further, the flow in the ramp broke down and became asymmetric resulting in a sharp decrease in drag and lift. Up to the point where the flow detached from the ramp, this was similar to the behaviour observed by Frost, although the peak C_L and C_D values were approximately 30% smaller in the Frost study.

Ruhrmann & Zhang (Ruhrmann and Zhang, 2003) further investigated diffuser flow using the model used in the present investigation, with end fences. Looking at the flow under the diffuser ramp, it was noted that for ramp angles of 10° and less, vortex breakdown was the cause of force reduction at small ride heights. This breakdown was strongly influenced by the underbody boundary layer. As the ramp angle was increased, the vortices were no longer strong enough to prevent flow separation on the ramp, and force reduction was caused by a combination of vortex breakdown and flow separation. Force reduction at these higher ramp angles was seen to exhibit hysteresis. The flow was observed to be unsteady after breakdown.

Although previous investigations into the vortical flow field generated by a diffuser equipped bluff body in ground effect exist, the streamwise evolution of the edge vortices and the influence of ride height has not been investigated. This investigation has applications in both automotive and aerospace aerodynamics. The evolution of a vortex in an adverse pressure gradient and any subsequent breakdown has applications to flap side edge aeroacoustics (Khorammi *et al*., 1999), a topic which is currently at the fore-front of aeroacoustics research. An additional application may be found in the validation of computational schemes such as detached eddy simulations (Kapadia *et al*., 2003) and large eddy simulations (Verzicco *et al*., 2002). The aims of this investigation are two-fold; a) to investigate the effect of ride height on the edge vortices generated by a diffuser equipped bluff body in ground effect, and b) to investigate the streamwise evolution of the edge vortices and identify any subsequent breakdown.

2. DESCRIPTION OF EXPERIMENTS

2.1 Wind Tunnel

The experimental investigations were performed in the 2.1m by 1.7m wind tunnel at the University of Southampton. The tunnel is of a conventional closed jet, closed circuit design and is equipped with a moving ground facility. In order for the ground plane to be correctly modelled a two-stage boundary layer removal system is located directly upstream of the moving ground. The majority of the boundary layer is scooped away using a vertical slot, aided by suction, and expelled outside the test section. The remainder of the boundary layer is removed using a horizontal, perforated plate across which suction is applied. This setup produces a velocity profile, perpendicular to the ground plane, which is equal to the freestream value at a height of 2mm, corresponding to $h_r/d < 0.013$. The freestream turbulence intensity within the test section is less than 0.2%.

2.2 Wind Tunnel Model

The model investigated is a generic bluff body 1.315m in length (l), 0.324m in height (h) and 0.157m in half-width (d), equipped with a rear diffuser. The start of the diffuser ramp is positioned 0.777m downstream of the nose of the model and extends downstream to the end of the model. Further details concerning the model design can be found in Senior & Zhang (Senior and Zhang, 2001).

The origin of the model was defined as the nose of the model with the Cartesian coordinate system set such that x was positive downstream, y was positive up and z was positive to port (Fig. 1(a)). The ride height (h_r) of the model was defined as the vertical distance between the ground plane and the start of the diffuser section. In order for the ride height to be continuously varied, with the model in situ, an automated motion and data logging system was used. The model was attached to the movement system via two struts, a main upstream strut and a lesser downstream pitch strut as shown in figure 1(b). Downforce and drag forces were obtained using a two-component load cell located between the main strut and the model.

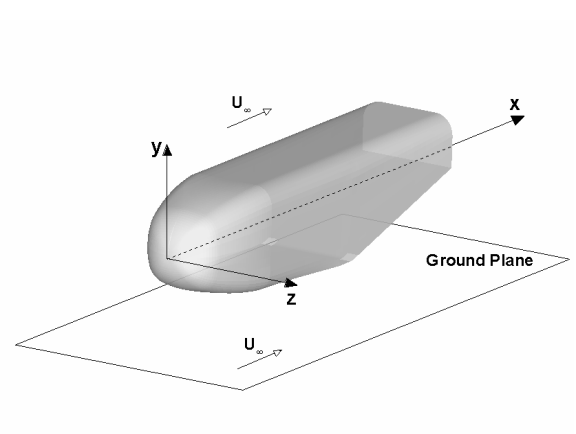

(a) Definition of the origin and coordinate system

(b) Model installation in the tunnel

Figure 1: Schematic of the test rig and installation within the wind tunnel

During all tests the model was positioned centrally, in a spanwise sense, within the test section and the yaw and pitch of the model were set at 0°. The ride height of the model was varied between 5mm (h_r/d=0.031) and 130mm (h_r/d=0.803). A wire 0.4mm in diameter was placed around the nose of the model at x=100mm in order to fix the boundary layer transition to turbulent and therefore ensure that transition occurred at the same located for each test. The wind and ground speeds were synchronized at a constant dynamic pressure of 56.25mm of water (U_8 ~30ms^{-1}) during all tests, corresponding to a Reynolds number (Re) of 2.7×10^6 based on the length of the model.

2.3 Experimental Procedures

Particle Image Velocimetry (PIV) was performed using a Dantec PowerFlow system, with the laser mounted outside the test section and the camera located directly downstream of the model. This setup allowed the flow field directly beneath the port edge of the diffuser to be investigated obtaining z-y planes at a fixed streamwise location. A diffuser expansion angle (?) of 10°, relative to the horizontal, was investigated since the force data obtained previously by Ruhrmann & Zhang (Ruhrmann and Zhang, 2003) indicated that a 10° expansion angle possessed features of both the high- and low-angle diffusers. The raw data obtained with the PIV system was analysed using a cross-correlation on a 32 by 32 pixel grid, a range validation of the resulting vectors generating a 157 by 125 grid and a moving average algorithm. A high resolution cross-correlation, using a 16 by 16 pixel region was performed at h_r/d=0.127 and x/d= 6.66. The location and size of the vortex did not change compared to the lower resolution cross-correlation, but the computational cost was increased significantly therefore a 32 by 32 cross-correlation was used for all the results presented in this paper.

The investigation into the port edge vortex and the corresponding flow field was two fold: a) the effect of ride height on the vortex was initially investigated at non-dimensional ride heights (h_r/d) of 0.045, 0.064, 0.096 and 0.127 at x/d= 8.38, and b) the streamwise evolution of the vortex was investigated at a non-dimensional ride height of 0.127 at x/d=5.81, 6.66, 7.52 and 8.38.

2.4 Errors and Uncertainties

The yaw and pitch of the model were set to within ±0.05°, and the ride height was set to within ±0.1mm. During all tests belt lift was not observed. The tunnel speed was run at a constant dynamic pressure of 56.25mm of water ±0.05mm (U_8 ~30ms^{-1}) in order for variations in density to be taken into account. Using procedures detailed by Moffet (Moffet, 1982) the errors in C_L and C_D were calculated using the addition method and a 95% confidence. The worst case was found to occur at a ride height of 0.318d, corresponding to a C_L of 0.7314±0.0024 and C_D of 0.3041±0.0017.

3. RESULTS AND DISCUSSION

3.1 Force Variations

Prior to investigating the flow field of the edge vortices the effects of ride height and diffuser expansion angle on the forces generated by the model were quantified. Figure 2 presents the variation in downforce (fig. 2(a)) and drag (fig. 2(b)) with non-dimensional ride height and diffuser expansion angle. For all ride heights, increasing the diffuser expansion angle resulted in an increase in both downforce and drag, with the exception of ?=5° and 10° at h_r/d=0.414 where the trend in reversed. Considering the ratio between the area at the diffuser inlet and the area at the diffuser exit it is clear that increasing the ramp angle will increase this ratio. In turn this increase in 'diffuser pumping' perturbates upstream increasing the mass flow rate beneath the model, as illustrated in the results of Ruhrmann & Zhang (Ruhrmann and Zhang, 2003), therefore increasing the downforce generated.

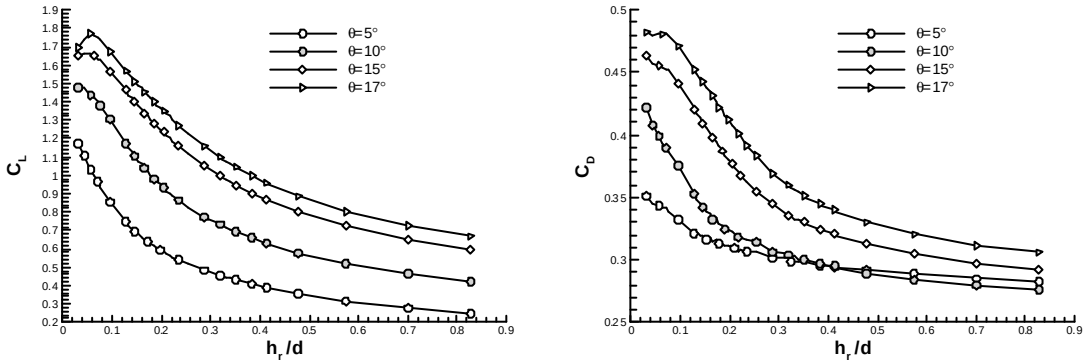

(a) Coefficient of Downforce (b) Coefficient of Drag

Figure 2: Variation in forces with non-dimensional ride height and diffuser expansion angle

Upon inspecting the variation in downforce with ride height a clear distinction between the behaviour of large divergence angles (15° and 17°) and the smallest divergence angle (5°) is observed. The 10° diffuser includes characteristics of both behaviour types. For non-dimensional ride heights above 0.0573, decreasing the ride height resulted in an asymptotic increase in downforce for all diffuser angles, referred to as the 'force enhancement region' by Senior & Zhang (Senior and Zhang, 2001). Ruhrmann & Zhang (Ruhrmann and Zhang, 2003) redefine this flow region as 'type a'. Decreasing the ride height results in a two-fold effect; 1) the flow underneath the model in accelerated more due to continuity effects, resulting in a decreased static pressure at the diffuser inlet (Ruhrmann and Zhang, 2003), which in turn causes, 2) the adverse pressure gradient within the diffuser to increase. The overall result is a more negative pressure within the diffuser and hence more downforce. With a 5° diffuser this force variation with ride height continues until a minimum value of ride height was achieved (h_r/d=0.0318).

Below a non-dimensional ride height of 0.0573 for diffuser angles of 15° and 17°, the downforce (C_L) reached a maximum value of 1.66 and 1.77 at ride heights of 0.0446d and 0.0573d respectively. Decreasing the ride height below this value resulted in the downforce decreasing, a trend which is more readily observed with a diffuser angle of 17°. Within previous research this force reduction has been

linked to the bursting of one vortex resulting in an asymmetric diffuser pattern (Senior and Zhang, 2001; Ruhrmann and Zhang, 2003), however the adverseness of the pressure gradients within those diffusers were large due to the presence of side fences. Since this case does not include side fences it can be assumed that the streamwise pressure gradients within the diffuser are less severe. Two possible explanations for this force behaviour exist. Firstly the ride height small enough such that the boundary layer on the underside of the model could essentially choke the diffuser inlet and therefore reduce the mass flow rate. Secondly the adverseness of the pressure gradients within the diffuser could be severe enough that either one or both of the vortices will breakdown.

The force variation with ride height for a diffuser angle of 10° possesses characteristics of both the high (15° and 17°) and low angle (5°) diffusers. A maximum value of downforce of 1.48 is observed at h_r/d=0.0446. Figure 3(a) presents an oil flow visualisation of the diffuser ramp at this maximum downforce ride height for a diffuser angle of 10°. Two vortices are indicates originating from the corners of the diffuser inlet. These expand as they move downstream along the ramp, moving inboard at the same time. A closed separation bubble, starting some distance from the diffuser inlet, is present in the centre of the ramp with the twin vortices bounding the edges of the separation bubble. While the vortices are expanding as they move downstream, there is no indication of vortex breakdown at this ride height.

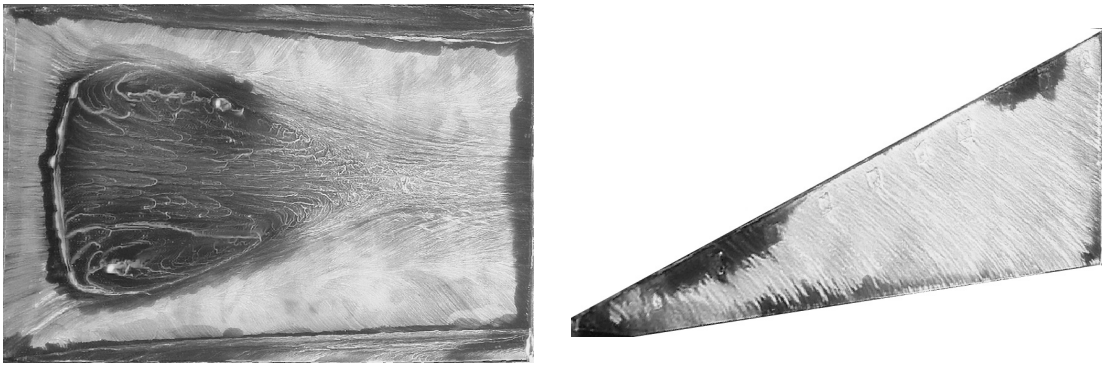

(a) Diffuser ramp (b) Port side of model

Figure 3: Oil flow visualisation at h_r/d=0.0446 with ?=10°, freestream flow from left to right

3.2 Effect of Ride Height on the Edge Vortex

The obtained forces have indicated that decreasing the ride height causes the diffuser flow field to alter creating two different flow regimes; a force enhancement and a force reduction region. In order to study the effect of ground proximity on the edge vortices PIV techniques were utilised allowing for streamwise slices of the vortex, and the associated vertical and spanwise velocities to be obtained. Figure 4 presents contours of non-dimensional vorticity (Ω) at the diffuser exit (x/d=8.38) at ride heights of 0.127d, 0.096d, 0.064d and 0.045d. Additional PIV surveys were obtained at x/d=5.81, 6.66 and 7.52 however the variations in vortex structure were less perceivable but did possess the same trends as those observed at x/d=8.38 and are therefore not presented in this paper.

At a ride height of 0.127d (fig. 4(a)) the edge vortex is readily observed, detached from the diffuser ramp, with a concentrated vortex core located inboard of the port side of the diffuser. The velocity vectors indicate that the vortex is formed by the flow on the port side of the model, which possesses a negative vertical component, separating from the surface. This observation is supported by the oil flow visualisation of the port side of the model (fig. 3(b)) which shows almost vertical surface streaklines at the port edge of the diffuser. Upon closer inspection of figure 4(a) a region of negative vorticity is present at the ground plane directly beneath the diffuser. It must be noted that although the ground plane possesses a velocity equal to freestream, the adverse pressure gradient generated by the diffuser will promote the growth of a boundary layer which is indicated by a region of negative vorticity in this instance.

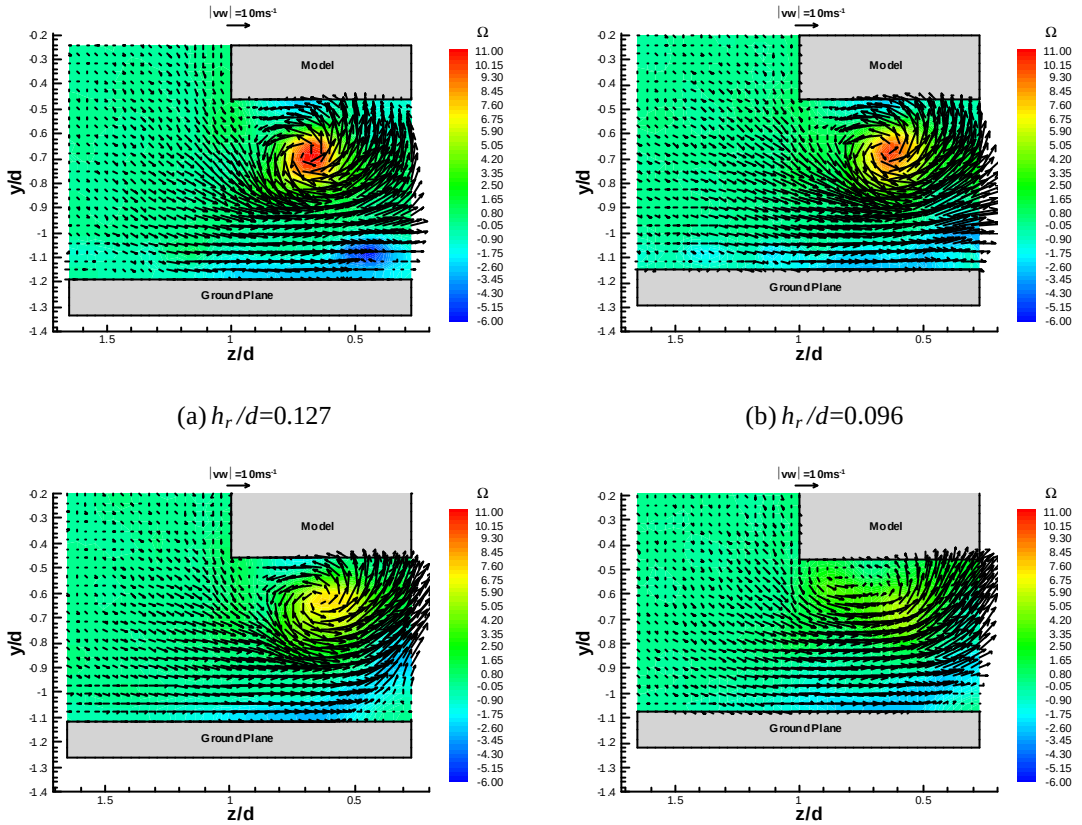

(a) h_r/d=0.127 (b) h_r/d=0.096

(c) h_r/d=0.064 (d) h_r/d=0.045

Figure 4: Contours of non-dimensional vorticity at x/d=8.38 various ride heights

Decreasing the ride height to 0.096*d* (fig. (b)) causes the vortex to become less concentrated, indicated by a reduction in vorticity within the vortex. The location and overall size of the vortex remains consistent with that observed at the higher ride height as does the size of the ground boundary layer. Further reductions in ride height to 0.064*d* (fig. 4(c)) cause the vortex core to seemingly breakdown, indicated by a dilation in the core (Lambourne and Brye, 1962), resulting in a region of anti-clockwise recirculation. The location of this recirculation remains consistent with the vortex core location observed at higher ride heights. At this ride height the ground boundary layer is seemingly separated from the ground and entrained into the region of recirculation towards the centre span of the diffuser. Figure 4(d) presents the flow field at the maximum downforce ride height of 0.045*d*. The vortex present at higher ride heights has undergone complete breakdown and is replaced by a region of weak anti-clockwise recirculation. The ground boundary layer is still entrained into the recirculation as before.

The PIV surveys of the port edge vortex have indicate that as the ride height is reduced the edge vortex becomes less concentrated and undergoes breakdown. As stated previously reducing the ride height caused the static pressure at the inlet of the diffuser to become more negative and hence the streamwise pressure gradient within the diffuser will become more adverse. This adverse pressure gradient will cause the vortex core to expand and the swirl component of the flow to decrease (Lucca-Negro and O'Doherty, 2001) which is observed as a reduction in vorticity. Therefore at a certain ride height the vortices within the diffuser will breakdown due to the streamwise pressure gradient becoming too adverse.

3.3 Streamwise Evolution of Edge Vortex

Figure 5 presents contours on non-dimensional vorticity at various streamwise locations along the diffuser (?=10°) at a ride height of 0.127*d*. At the most upstream location of *x/d*=5.81 (fig. 5(a)) the freestream flow is entrained into the diffuser causing the flow to separate off the edge of the diffuser. A region of recirculation in observed attached to the ramp of the diffuser, with the centre of the recirculation located at *y/d*=-1.02 and *z/d*=0.87. A region of weak negative vorticity directly beneath the diffuser just above the ground plane is observed, corresponding to the ground boundary layer described previously. Moving downstream to *x/d*=6.66 (fig. 5(b)) results in the region of recirculation becoming stronger and moving inboard (*z/d*=0.78) while still attached to the diffuser ramp. The ground boundary layer has grown in height but still remains attached to the ground plane.

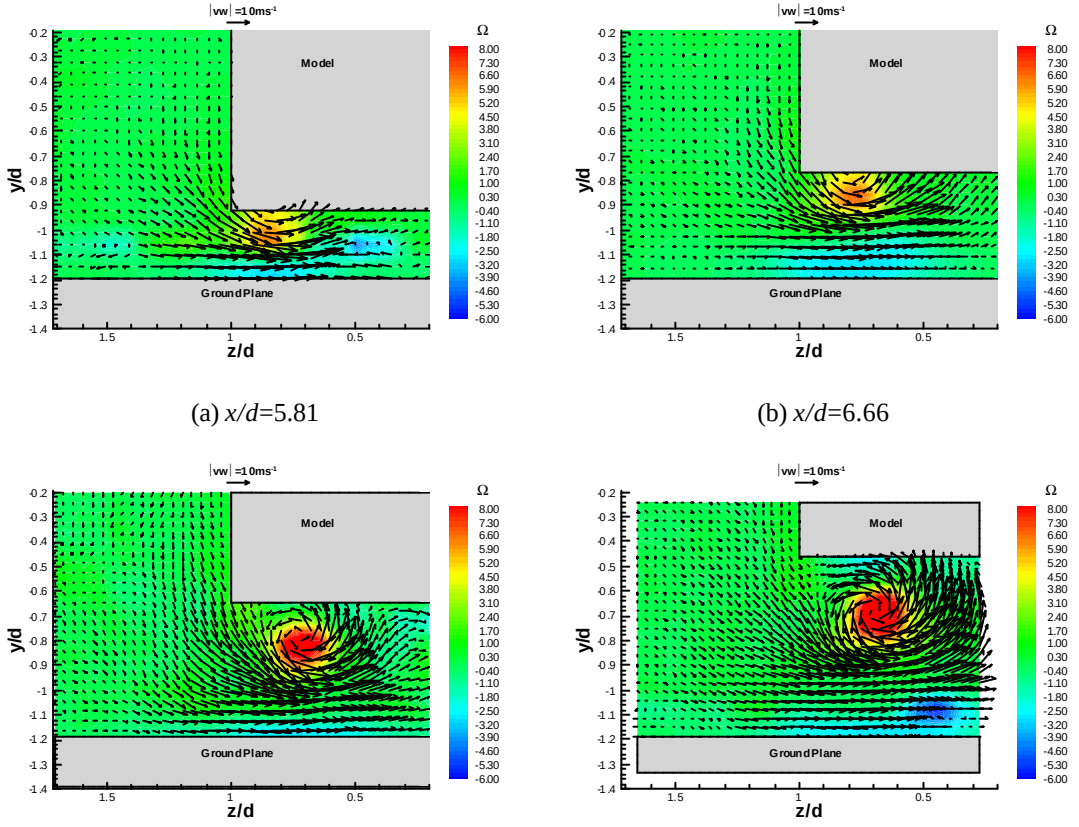

(a) *x/d*=5.81

(b) *x/d*=6.66

(c) *x/d*=7.52

(d) *x/d*=8.38

Figure 5: Contours of non-dimensional vorticity at h_r/d=0.127

The flow field observed at *x/d*=7.52 (fig. 5(c)) indicates the presence of a concentrated vortex detached from the diffuser ramp. The vortex core is located at *y/d*=-0.82 and *z/d*=0.71 indicating that it has moved inboard and upwards when compared to more upstream locations. At the exit of the diffuser (fig. 5(d)) a strong concentrated vortex is observed with the core seemingly expanded. The core of the vortex has moved inboard and upward while the vertical distance between the vortex and the diffuser ramp has increased. The ground boundary layer remains completely attached to the ground plane.

The streamwise location of the vortex core and the variations in vertical and spanwise location are presented in figure 6. Seven ride heights ranging from 0.127*d* to 0.032*d* are presented. The inboard and upward movement of the vortex is clearly indicated which remains relatively independent of ride height.

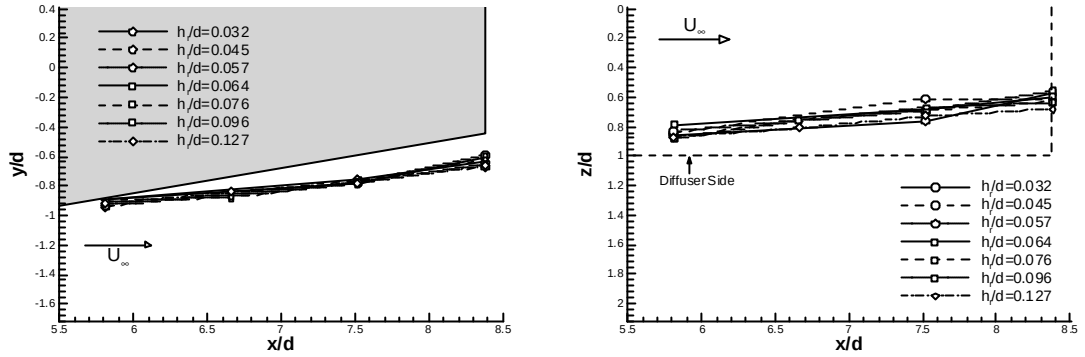

(a) Vertical location (b) Spanwise location

Figure 6: Streamwise location of the port vortex core at various ride heights

The PIV surveys at various streamwise locations indicate that the edge vortex evolves from a weak region of recirculation attached to the diffuser ramp, into a strong detached concentrated vortex. Near the inlet of the diffuser the physical space between the diffuser ramp and the ground plane is small constraining the swirl of the flow and hence limiting the size and strength of the recirculation region. As the distance between the diffuser ramp and the ground plane increases, i.e. an increase in streamwise location, the flow is less constrained and can therefore generate a vortex detached from the model. The PIV surveys in figure 5 indicate that the vortex does not undergo breakdown since the streamwise pressure gradient is not adverse enough. However it has been shown that reducing the ride height causes the vortex to breakdown (fig. 4). It could therefore be hypothesized that reducing the ride height would alter the evolution of the vortex in such a way as to promote breakdown prior to the exit of the diffuser.

4. SUMMARY REMARKS

The generation, evolution and in certain cases breakdown of the edge vortices generated by a diffuser equipped bluff body have been experimentally investigated. PIV, force and oil flow visualisation techniques were used in conjunction, to analyse the flow field and any variations due to ride height. The forces indicate that the edge vortices enhance the downforce as the ride height is reduced until a maximum value of downforce is achieved. Beyond this point the downforce decreases due to the edge vortices breaking down as a result of the adverse pressure gradient within the diffuser becoming too severe. At large values of ride height the edge vortices are generated close to the inlet of the diffuser and are attached to the diffuser ramp. Further downstream the vortices evolve to become concentrated and detached from the diffuser ramp, moving inboard as they evolve. It is hypothesized that at lower values of ride height the edge vortices do not evolve properly and undergo breakdown prior to the exit of the diffuser.

ACKNOWLEDGEMENTS

The authors wish to thank Andreas Rurhmann, Willem Toet and BARf1 for the technical support and the manufacture of the model investigated.

REFERENCES

Frost, R.L.L. (1981), “Experimental investigations of the base pressures found on a bluff body in ground effect”, Aeronautical Journal, Feb., pp. 63-70

George, A.R. (1981), “Aerodynamic effects of shape, camber, pitch and ground proximity on idealized ground vehicle bodies”, Journal of Fluids Engineering, 103, pp. 631 – 638

Cooper, K.R., Bertenyi, T., Dutil, G., Syms, J. and Sovran, G. (1998), "The aerodynamic performance of automotive underbody diffusers", SAE Paper 980030

Cooper, K.R., Sovran, G. and Syms, J. (2000), "Selecting automotive diffusers to maximise underbody downforce", SAE Paper 2000-01-0354

Senior, A.E. & Zhang, X. (2001), "The force and pressure of a diffuser-equipped bluff body in ground effect", Journal of Fluids Engineering, 123, (1), pp. 105-123

Rurhmann, A., & Zhang, X. (2003), "Influence of diffuser angle on a bluff body in ground effect", Journal of Fluids Engineering, 125, (2), pp. 332-338

Burgin, K., Adey, P.C., Beatham, J.P. (1986), "Wind tunnel tests on road vehicle models using a moving belt simulation of ground effect", Journal of Wind Engineering and Industrial Aerodynamics, 22, pp. 227 – 236

Khorammi, M.R., Singer, B.A., and Radeztsky, R.H. Jr. (1999), "Reynolds-Averaged Navier-Stokes computations of a flap-side-edge-flowfield", AIAA Journal, 37, (1), pp. 14-22

Kapadia, S., Roy, S. and Wurtzler, K. (2003), "Detched eddy simulation over a reference Ahmed car model", AIAA Paper 2003-0857, 41st Aerospace Sciences Meeting & Exhibit, Reno, Navada, 6-9 January.

Verzicco, R., Fatica, M., Iaccarino, G., Moin, P. and Khalighi, B. (2002), "Large eddy simulation of a road vehicle with drag-reduction devices", AIAA Journal, 40, (12), pp. 2447-2455

Moffet, R. (1982), "Contributions to the theory of single-sample uncertainty analysis", Journal of Fluids Engineering, 104, pp. 250-260

Lambourne, N.C. and Bryer, D.W. (1962), "The bursting of leading-edge vortices-some observations and discussion of the phenomenon", Aeronautical Research Council, R&M No. 3282

Lucca-Negro, O. and O'Doherty, T. (2001), "Vortex breakdown: a review", Progress in energy and combustion science, 27, pp. 431-481